JACS
JOURNAL OF THE AMERICAN CHEMICAL SOCIETY

Article

pubs.acs.org/JACS

Oligomer Formation of the Bacterial Second Messenger c-di-GMP: Reaction Rates and Equilibrium Constants Indicate a Monomeric State at Physiological Concentrations

Martin Gentner, Martin G. Allan,[§] Franziska Zaehringer, Tilman Schirmer,* and Stephan Grzesiek*

Biozentrum, University of Basel, Klingelbergstrasse 50/70, 4056 Basel, Switzerland

Supporting Information

ABSTRACT: Cyclic diguanosine-monophosphate (c-di-GMP) is a bacterial signaling molecule that triggers a switch from motile to sessile bacterial lifestyles. This mechanism is of considerable pharmaceutical interest, since it is related to bacterial virulence, biofilm formation, and persistence of infection. Previously, c-di-GMP has been reported to display a rich polymorphism of various oligomeric forms at millimolar concentrations, which differ in base stacking and G-quartet interactions. Here, we have analyzed the equilibrium and exchange kinetics between these various forms by NMR spectroscopy. We find that the association of the monomer into a dimeric form is in fast exchange (<milliseconds) with an equilibrium constant of about 1 mM. At concentrations above 100 μM, higher oligomers are formed in the presence of cations. These are presumably tetramers and octamers, with octamers dominating above about 0.5 mM. Thus, at the low micromolar concentrations of the cellular environment and in the absence of additional compounds that stabilize oligomers, c-di-GMP should be predominantly monomeric. This finding has important implications for the understanding of c-di-GMP recognition by protein receptors. In contrast to the monomer/dimer exchange, formation and dissociation of higher oligomers occurs on a time scale of several hours to days. The time course can be described quantitatively by a simple kinetic model where tetramers are intermediates of octamer formation. The extremely slow oligomer dissociation may generate severe artifacts in biological experiments when c-di-GMP is diluted from concentrated stock solution. We present a simple method to quantify c-di-GMP monomers and oligomers from UV spectra and a procedure to dissolve the unwanted oligomers by an annealing step.

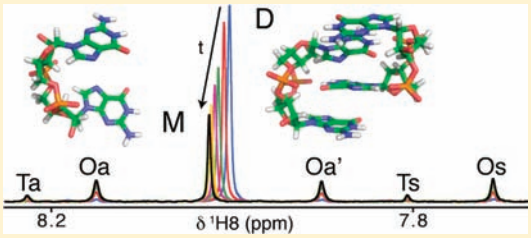

INTRODUCTION

Cyclic diguanosine-monophosphate (c-di-GMP) has emerged as a second messenger that is used by most bacteria to regulate a switch between a free-living, planktonic and a sedentary, biofilm-related lifestyle.[1] In pathogenic bacteria, these two lifestyles are correlated with virulence and persistence of infection. Presumably due to the low cellular concentration of c-di-GMP in the micromolar range,[2] the ubiquitous presence of this second messenger has only been recognized recently and indirectly from the identification of genes coding for c-di-GMP-associated enzymes in almost all bacterial genomes. In particular, diguanylate cyclases (GGDEF domain proteins) and c-di-GMP-specific phosphodiesterases (EAL and HD-GYP proteins) are commonly found as several variants. Molecular aspects of c-di-GMP signaling have been recently reviewed.[3,4]

C-di-GMP is a C_2-symmetric molecule that consists of a 12-membered macrocycle formed by the ribose and phosphate moieties and two guanine groups (Figure 1A). Several structures have been determined by X-ray crystallography, in both free (Figure 1B)[5−7] and protein-bound forms.[3] They show similar conformations for the macrocycle, with both phosphodiester torsion angles α/β in gauche(+)/gauche(+) conformation.[5] Thus, the backbone of the molecule appears rather constrained. Interestingly, in all aforementioned small-molecule structural studies, c-di-GMP is in dimeric form with intercalated bases and inter-monomeric H-bonding between the guanine N1 and the phosphate groups. Similar dimeric forms have also been reported for c-di-AMP.[8] In some cases, the c-di-GMP dimers coordinate Mg^{2+} or Co^{2+} ions by the N7 atoms of the two central bases, but this does not significantly change the structure.[5,6] The same intercalated c-di-GMP dimer has also been observed in protein complexes, where it binds to the allosteric inhibition site of diguanylate cyclases,[9,10] to PilZ receptors,[11,12] and a response regulator.[13] This prompted the notion that the biologically active species may be dimeric,[14] although for degradation c-di-GMP binds in monomeric form to EAL phosphodiesterases.[15−17] A structure of a PilZ protein with monomeric c-di-GMP has also been reported.[18]

Previous NMR studies on c-di-GMP in solution have been performed only at high (>1 mM) concentrations,[19−21] revealing a rich polymorphism, ranging from dimers to several forms of higher oligomers in a cation-dependent equilibrium. Interestingly, no such polymorphs are observed for a circular trinucleotide of GMP.[22] The higher oligomeric species have been assigned to tetramers and octamers on the basis of UV, CD, NOE, and diffusion experiments.[21] However, the detailed structures of the tetramers and octamers are unknown. For the

Received: August 16, 2011
Published: December 5, 2011

   dx.doi.org/10.1021/ja207742q | J. Am. Chem.Soc. 2012, 134, 1019−1029

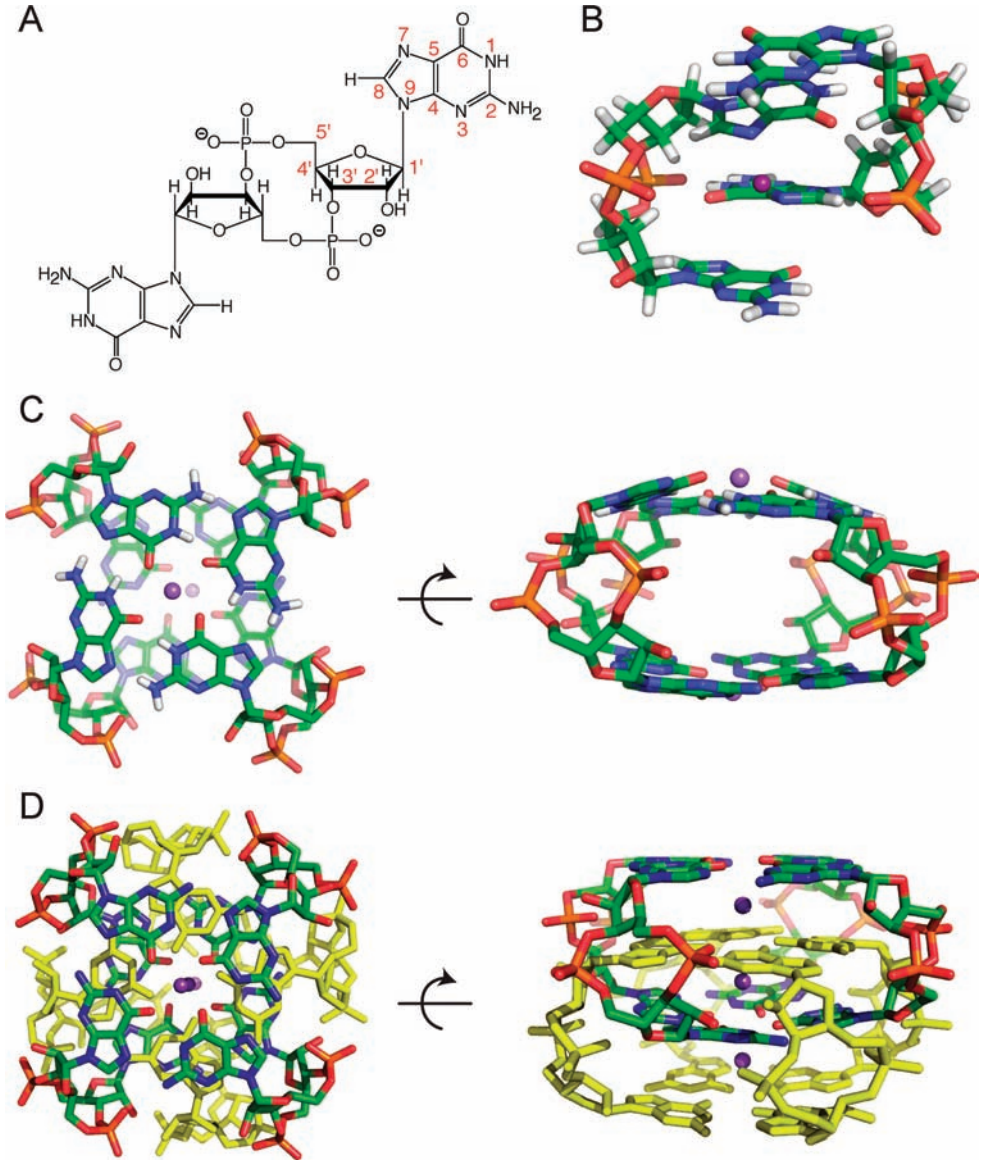

Figure 1. Chemical structure and three-dimensional models of c-di-GMP. (A) Chemical structure and atom numbering of monomeric c-di-GMP in *anti* conformation. (B) Crystal structure of dimeric c-di-GMP in the presence of magnesium, adapted from Egli.[5] (C) Modeled structure of tetrameric c-di-GMP forming two G-quartets in *anti* conformation, based on the schemes proposed by Zhang.[21] Complexed Na^+ cations are shown within each of the G-quartets. (D) Modeled structure of all-*anti* octameric c-di-GMP[21] in the presence of three Na^+ ions between adjacent G-quartets. The intercalated molecules are displayed as yellow sticks for clarity.

tetramer, a cage-like four-fold symmetric structure has been proposed[7,21] with the two guanine bases of one c-di-GMP monomer contributing to two parallel, but not stacked, quartets. Figure 1C presents an energy-minimized model structure of such a tetramer. The octamer was proposed to consist of two intercalated tetramers.[21] Modeling (Figure 1D) shows that in order to prevent steric clashes, the two intercalating tetramers need to be shifted relative to each other by about half the tetramer height and rotated by about 45° on the common four-fold symmetry axis. This results in a closely packed assembly with four stacked guanine quartets stabilized by monovalent cations situated on the symmetry axis.[23] A recent study revealed that c-di-GMP polymorphism critically depends on the phosphate linkage, since substitution of one of the 5′ oxygens by sulfur leads to a diminished propensity to form oligomers.[19] In contrast to the clear experimental evidence for higher oligomeric forms at millimolar c-di-GMP concentrations, the presence of G-quartets at micromolar concentrations has only been inferred from CD, fluorescence, and absorbance data when additional aromatic intercalators were present.[6,24,25]

The current study aimed to determine the state of c-di-GMP at physiological, i.e., micromolar, concentrations in various buffer conditions. During the study, it became apparent that c-di-GMP exhibits extremely slow kinetics of oligomer formation and dissociation in the presence of metal ions. Slow kinetics have been observed before for G-quartet formation from larger DNA oligomers,[26] but no analysis exists of c-di-GMP oligomer formation. Here, we have determined kinetic parameters and equilibrium constants for c-di-GMP monomer, dimer, tetramer, and octamer exchange in detail. The results indicate that c-di-GMP is monomeric at physiologically low concentrations. However, due to the extremely slow exchange kinetics, care must be taken to reach equilibrium conditions during *in vitro*

dx.doi.org/10.1021/ja207742q | *J. Am. Chem.Soc.* 2012, 134, 1019–1029

experiments. Simple methods are presented to quantify the amount of oligomeric state by UV absorbance and to dissociate the oligomers by annealing.

MATERIALS AND METHODS

Modeling of c-di-GMP Oligomers. Models of c-di-GMP tetramers and octamers were built manually on the basis of the high-resolution crystal structure[23] (PDB code 352d) of a parallel-stranded Na^+/guanine tetraplex. The models were energy minimized with REFMAC5[27] employing restraints on the interbase H-bond distances (2.8 Å) and the Na^+−O6 distances (2.0 and 3.0 Å, in the case of the tetramer and octamer, respectively).

Sample Preparation. Purified c-di-GMP was produced as described previously by enzymatic synthesis from GTP.[28] In order to mimic cytosolic salt and pH conditions,[29] c-di-GMP was dissolved in 250 mM KCl, 5 mM Na_2HPO_4/NaH_2PO_4, pH 7.4, 5% D_2O in the presence of either 10 mM Na_2EDTA (buffer A) or 10 mM $MgCl_2$ (buffer B). To investigate c-di-GMP in the absence of cations, c-di-GMP was also dissolved in 5 mM TRIS/HCl (tris(hydroxymethyl)-aminomethane, HCl salt), pH 8.0, 5% D_2O (buffer C). Samples were then transferred into 5 mm standard NMR tubes (volume >400 μL) for low c-di-GMP concentrations (<2 mM) or Shigemi tubes (270 μL) at higher concentrations.

1D NMR Spectroscopy. Unless indicated otherwise, samples were heated to 60 °C for at least 1 h to facilitate the dissociation of oligomers prior to measurements and kept at room temperature for 1 h before NMR measurements. NMR experiments were carried out on a Bruker Avance DRX 600 spectrometer equipped with a triple-resonance pulse field gradient probe head (TXI) at a temperature of 24 °C. 1D proton NMR spectra were recorded with the proton carrier set on water and the excitation sculpting scheme[30] achieving water suppression by gradient dephasing. Spectra were recorded as 57 344 complex points with an acquisition time of 1.99 s and a recovery delay of 1 s. Total NMR experiment times ranged from 6 min to 15 h, depending on the c-di-GMP concentration (~10 mM to ~0.5 μM, respectively). Spectra were processed and evaluated using Topspin 2.1.6 (Bruker). Chemical shifts were determined relative to external trimethylsilyl-2,2,3,3-tetradeuteriopropionic acid in water (pH 7).

Determination of c-di-GMP Concentrations. Due to the hypochromic effect upon oligomerization (see below), c-di-GMP concentrations were determined not by UV absorption measurements but by comparing NMR peak intensities (normalized on the number of scans and on the proton 90° hard pulse length)[31] to the intensity of a reference GTP sample. More specifically, the peak integrals of the well-separated, aromatic H8 resonances were compared to the integral of the GTP H8 resonance (50 μM) in the identical buffer. Very similar results were obtained when H1′ resonances were used for quantification. The concentration of the GTP sample was determined by UV measurement at 253 nm using a molar extinction coefficient of 13 700 M^{-1} cm^{-1}.[32] The investigated c-di-GMP concentration ranges were 0.5 μM−6 mM (buffers A and B) and 1 μM−10 mM (buffer C). UV measurements were carried out in quartz cuvettes (Hellma) with a path length of 1 cm on an HP/Agilent 8453 spectrophotometer or a Varian Cary 50 spectrophotometer.

To exclude that oligomer formation would affect the GTP reference, we compared NMR spectra of 100 μM and 50 μM GTP dissolved in buffer A (Figure S9). Neither oligomer resonances nor any resonance shifts were observed. Repeated measurements after more than 10 days revealed less than 2% changes in both H8 and H1′ resonance integrals. Thus the effects of GTP oligomerization and H/D exchange are negligible.

Determination of c-di-GMP Dimer Dissociation Constants. C-di-GMP monomer and dimer were observed in fast chemical exchange on the chemical shift time scale, leading to a single set of resonances for monomer and dimer. We denote this combined spectral species as MD. The experimentally observed chemical shifts for MD (δ_{MD}) represent the population-weighted mean,

$$\delta_{MD} = \frac{[M]\delta_M + 2[D]\delta_D}{[M] + 2[D]} = \frac{[M]\delta_M + 2[D]\delta_D}{[MD]} \quad (1)$$

where δ_M, δ_D are the chemical shifts and [M], [D] the concentrations of monomers and dimers, respectively, and [MD] = [M] + 2[D] is the concentration of monomers plus dimers (in monomeric units). Since the dimer dissociation constant K_{MD} is defined as

$$K_{MD} = \frac{[M]^2}{[D]} \quad (2)$$

the monomer concentration can be expressed as a function of K_{MD} and [MD] as

$$[M] = -\frac{K_{MD}}{4} + \sqrt{\left(\frac{K_{MD}}{4}\right)^2 + \frac{[MD]K_{MD}}{2}} \quad (3)$$

Substitution into eq 1 then yields the calculated shift for the MD resonance (δ_{calc}) as a function of [MD], K_{MD}, δ_M, and δ_D. The unknown parameters (K_{MD} and δ_D) were determined by fitting δ_{calc} to the experimentally determined chemical shift δ_{exp} (H8 resonance) via minimization of the target function,

$$\chi^2 = \sum_i \left(\frac{\delta_{exp,i} - \delta_{calc,i}(K_{MD}, [MD])}{\sigma_i}\right)^2 \quad (4)$$

by an in-house-written Matlab (MathWorks) routine. Errors in the fit parameters were determined by a Monte Carlo procedure.

Modeling of Kinetic Parameters. The time courses of oligomer concentrations were modeled according to the kinetic scheme given in Figure 6. The coupled differential equations for the concentrations of the slowly interconverting monomers, tetramers, and octamers were assumed as

$$\begin{aligned} d[M]/dt &= -4k_{TM}[M]^4 + 4k_{MT}[T] \\ &\quad - 4k_{OT}[T][M]^4 + 4k_{TO}[O] \\ d[T]/dt &= k_{TM}[M]^4 - k_{MT}[T] - k_{OT}[T][M]^4 \\ &\quad + k_{TO}[O] \\ d[O]/dt &= k_{OT}[T][M]^4 - k_{TO}[O] \end{aligned} \quad (5)$$

with k_{BA} representing the rate of the A→B reaction.

Since, the monomer/dimer reaction is fast on the time scale of these reactions, the [M] and [D] concentrations were assumed to be in instant equilibrium according to eq 2 during the simulations. Furthermore, the equally populated but spectroscopically distinct two tetrameric species (Ts, Ta) and three octameric species (Os, Oa, Oa′) were subsumed into single tetrameric and octameric concentrations, such that [Ts] = [Ta] = [T]/2 and [Os] = [Oa] = [Oa′] = [O]/3.

The differential equations were integrated numerically using the program ProFit (Quansoft, Zürich). Non-uniform time steps were used such that the change in concentration of each species was not larger than 0.1%. Forward and backward rates of reactions M⇄T and T⇄O as well as the boundary conditions for the concentrations at time $t = 0$ were then obtained by fitting the integrated time courses to the observed data using the same program. Since the sum of the observed NMR concentrations ($\sum_{obs}$) of the identified species was not constant, but decreased (Figure 4B) or increased (Figure 5A) slightly with time (presumably due to the formation or dissociation of higher, unobservable oligomers, see below), the total c-di-GMP concentration $[c\text{-di-GMP}]_t$ was adjusted for each time point to the value obtained by fitting $\sum_{obs}$ to an exponential function. Errors in the fit parameters were determined by a Monte Carlo procedure.

Modeling of Time-Dependent UV Absorption Spectra. The behavior of the UV absorption spectrum $A(\lambda)$ of a c-di-GMP sample after dilution was modeled as a linear combination of absorption spectra from the unstacked (monomeric) form $A_{mono}(\lambda)$ and a second,

dx.doi.org/10.1021/ja207742q | J. Am. Chem.Soc. 2012, 134, 1019−1029

distinct spectrum of a stacked form $A_{stacked}(\lambda)$, such that

$$A(\lambda) = A_{mono}(\lambda)p_{mono} + A_{stacked}(\lambda)(1 - p_{mono}) \quad (6)$$

where the population of the monomeric form p_{mono} was derived from the NMR intensity and frequency position of the H8 proton. The component, modeled absorption spectra $A_{mono}(\lambda)$ and $A_{stacked}(\lambda)$ were then obtained by a linear fit of eq 6 to experimental absorption spectra acquired a different time points after dilution.

RESULTS AND DISCUSSION

1D NMR Spectra of c-di-GMP at Various Concentrations. In the presence of metal cations, complex polymorphism of c-di-GMP has been observed at high millimolar concentrations previously by NMR spectroscopy.[20,21] Here we have addressed the question of the c-di-GMP oligomerization state at conditions that resemble the physiological environment with respect to c-di-GMP concentration, salt, pH, and temperature or at conditions used routinely for the functional *in vitro* characterization of c-di-GMP-related enzymes.

C-di-GMP under Physiological Salt and pH Conditions. Figure 2A,B shows the H1, H8, and H1′ parts of c-di-GMP ^{1}H spectra at various concentrations ranging from 19 μM to 1 mM in buffer A (250 mM KCl, 5 mM Na_2HPO_4/NaH_2PO_4, 10 mM Na_2EDTA, pH 7.4), which was chosen to mimic the salt concentrations and pH of the bacterial cytosol.[29] At a concentration of 1 mM, c-di-GMP exhibits several resonances for the H1, H8, and H1′ protons as well as for the other aliphatic ribose protons (not shown). Zhang et al.[20,21] have observed similarly complex spectra at high (>30 mM) c-di-GMP concentration in the presence of monovalent cations. This spectral heterogeneity was attributed to several oligomeric species comprising an intercalated dimer, as well as several types of tetramers and octamers. The propensity of oligomer formation was much more pronounced for K^+ than for Li^+ and Na^+ cations.

It is apparent from Figure 2B that the frequencies of the tetramer and octamer resonances remain constant with varying c-di-GMP concentration, whereas their relative intensities change. Hence these species are in slow exchange on the chemical shift time scale, i.e., significantly slower than about 17 ms, which corresponds to the inverse of their ~0.1 ppm frequency separation. In contrast, a number of resonances exhibit concentration-dependent shift changes. This is exemplified for the H8 resonance in Figure 2B. We attribute this set of resonances to c-di-GMP monomers and dimers, designated as MD, which are in fast exchange on the chemical shift scale. Since the resonances are not significantly broadened, the exchange must be considerably faster than about 34 ms, corresponding to a frequency separation of at least 0.05 ppm. It is also noted that, in contrast to tetramers and octamers, no imino proton H1 resonance is observed for the MD species. This indicates the absence of H-bonding and rapid exchange with the solvent. In a previous study,[21] this set of MD resonances had been attributed to an intercalated dimer in *anti* conformation that exchanges with an unstructured form. However, the exchange had not been characterized further.

We also investigated whether the presence of divalent cations had an influence on the observed oligomer formation. For this purpose, the experiments were repeated in the presence of magnesium in buffer B (250 mM KCl, 5 mM Na_2HPO_4/NaH_2PO_4, 10 mM $MgCl_2$, pH 7.4). A behavior very similar to that for buffer A was observed (Figure S1). Thus magnesium does not significantly influence the oligomerization process.

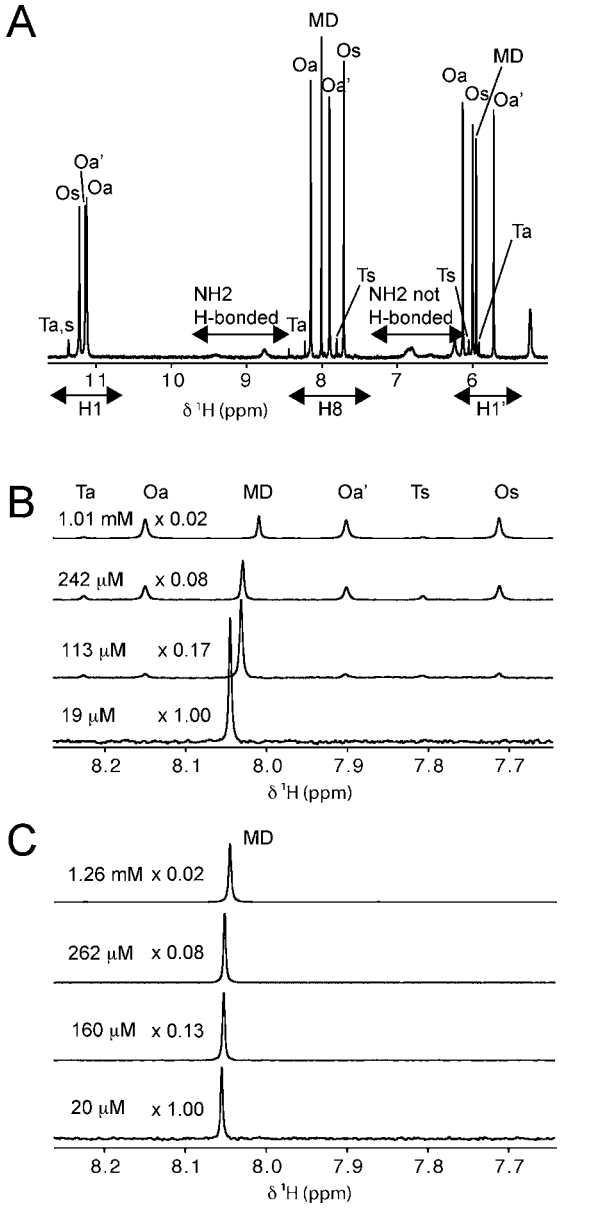

Figure 2. 1D ^{1}H NMR spectra of c-di-GMP. (A) H1, H8, and H1′ resonances of 1.0 mM c-di-GMP dissolved in buffer A. Resonance assignments for tetramers (Ta, Ts) and octamers (Oa, Oa′, Os) were taken from Zhang.[21] MD resonances represent the population-weighted mean chemical shift of rapidly exchanging monomers and dimers. (B) H8 region of the spectrum at various c-di-GMP concentrations in buffer A. Indicated c-di-GMP concentrations were obtained from the sum of the assigned H8 c-di-GMP peak intensities (see text). (C) Same as (B) but c-di-GMP was dissolved in buffer C.

c-di-GMP in TRIS Buffer. To study c-di-GMP oligomerization behavior also for conditions routinely used in enzymatic assays, the experiments were repeated in buffer C (5 mM TRIS/HCl, pH 8) containing no metal cations. Figure 2C shows the H8 part of the c-di-GMP ^{1}H spectrum at various concentrations. In contrast to buffer A (Figure 2B), only a single H8 resonance is detected in the concentration range from 20 μM to 1.26 mM and even at 10 mM c-di-GMP (not shown). Also, none of the other c-di-GMP resonances show any sign of heterogeneity. In addition, and in contrast to the tetrameric and octameric forms in the presence of cations, no imino H1 resonances are observed in buffer C even at high

dx.doi.org/10.1021/ja207742q | J. Am. Chem.Soc. 2012, 134, 1019–1029

concentrations. This again indicates the absence of a stable H-bond and rapid exchange with the solvent. The resonances are very similar to the MD resonances in buffers A and B and also shift in a concentration-dependent manner. Hence, they were attributed to the MD species, which is in rapid exchange between monomer and dimer. We also tested the effect of phosphate on oligomerization. A solution of 1 mM c-di-GMP in 5 mM TRIS/HCl, 150 mM KCl, pH 8, devoid of phosphate showed oligomer (T, O) resonances very similar to those observed for c-di-GMP dissolved in buffers A and B (Figure S10). Thus, the lack of phosphate is not responsible for the absence of oligomers in buffer C. To assay the effect of different monovalent cations, further samples of 1 mM c-di-GMP dissolved in 5 mM TRIS/HCl were prepared in the presence of large concentrations (≥150 mM) of either KCl, NaCl, or LiCl. Only for KCl, oligomer formation was observed (Figure S10). Thus, Li^+ and Na^+ seem to have a much lower potential to induce oligomerization of c-di-GMP at low millimolar concentrations, although for higher concentrations some coordination of Li^+ and Na^+ has been reported.[20,21] Altogether, this indicates that for concentrations up to at least 1 mM and in the absence of the tested metal ions, c-di-GMP does not form oligomers beyond the dimer. This is consistent with the observation that all described G-quartet structures are stabilized by the coordination of monovalent cations.[20,21,33−35]

c-di-GMP Monomer/Dimer Equilibrium. To determine equilibrium constants and exchange rates of the different oligomeric c-di-GMP forms, the frequency positions and resonance intensities of the well-isolated H8 proton were analyzed in a quantitative manner. Figure 3A,B (left side) shows the chemical shift of the MD resonance as function of the total c-di-GMP concentration for buffers A and B, respectively. For fast monomer/dimer exchange, the shift would be expected to show a sigmoidal dependence on the concentration. However, very large scatter and multiphasic behavior were observed. This was traced back to the very slow exchange kinetics (see below) between the MD species and the higher oligomeric forms, which did not reach equilibrium after dilution from stock solutions even after extended periods of several days at room temperature.

To determine the total MD concentration in the absence of an overall equilibrium with the higher oligomers, the integral of the MD H8 resonance was used as a measure. This intensity was calibrated to an absolute concentration by comparison to the integral of the H8 resonance of GTP, determined in a separate experiment with the GTP concentration defined by UV absorbance. Figure 3A,B (right side) shows the H8 chemical shift as a function of this calibrated MD concentration. It is obvious that there is much less scatter and that the dependence becomes monophasic.

At low (<10 μM) total c-di-GMP concentration, the chemical shift value of the H8 MD resonance converges to the chemical shift of the free monomer at 8.050 and 8.054 ppm in buffers A and B, respectively. With increasing concentration the resonance shifts upfield, i.e., toward the chemical shift of the dimer. However, within the investigated concentration range of up to 6 mM, the shift does not converge to a constant, and hence the dimeric state is not fully reached. Apparently, this is due to the onset of higher oligomer formation above about 20−100 μM total c-di-GMP concentration (depending on buffer conditions), which diminishes the total available MD concentration. Fitting of the chemical shift dependence to a simple monomer/dimer equilibrium yielded dimer dissociation

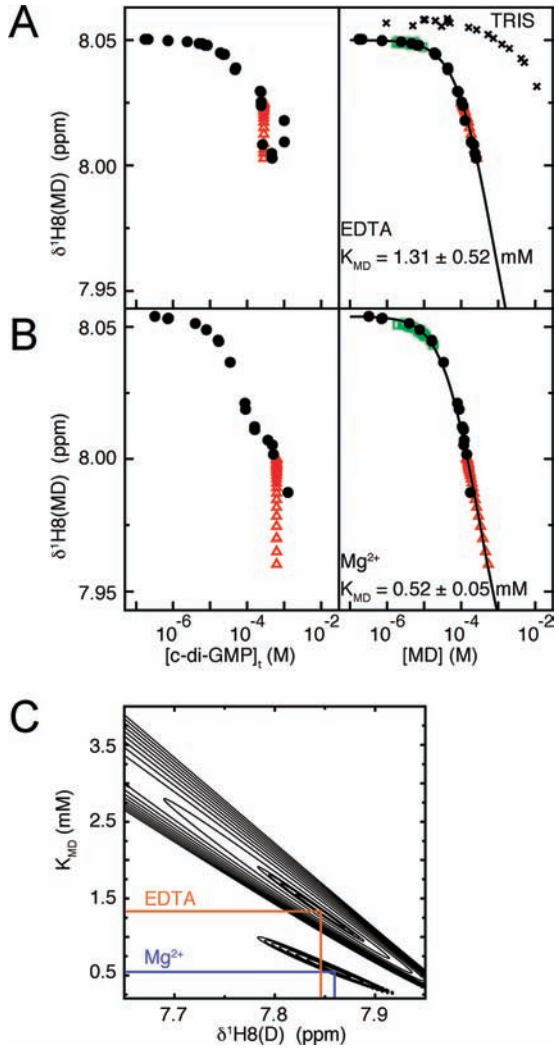

Figure 3. Concentration dependence of the c-di-GMP monomer/dimer equilibrium as evidenced from the chemical shift of the MD H8 resonance. (A) H8 chemical shift of c-di-GMP in buffer A as function of total c-di-GMP concentration $[c\text{-di-GMP}]_t$ (left) and combined monomer/dimer concentration [MD] as determined from the H8 peak intensity (right). (B) same as (A) but spectra were recorded in buffer B. Filled black circles in (A) and (B) represent data from a titration experiment, while red triangles and green squares indicate data from oligomer reassociation (Figure 4) and dilution experiments (Figure 5), respectively. Black crosses in panel A (right) depict data from a titration of c-di-GMP in buffer C. The solid lines in (A) and (B) represent fits to a two-state model according to eq 1. (C) Mean-square deviation χ^2 of fitted and experimental shifts according to eq 4 as a function of the fit parameters K_{MD}, δ_D(H8) for buffers A (EDTA) and B (Mg^{2+}).

constants of 1.31 ± 0.52 and 0.52 ± 0.05 mM in buffers A and B, respectively. Since the dimer chemical shift δ_D could not be determined experimentally, the accuracy of the resulting dissociation constant is limited, as the fit parameters K_{MD} and δ_D are strongly coupled. This is demonstrated by the elongated minima in a $\chi^2(K_{MD},\delta_D)$ plot (Figure 3C). Despite this uncertainty, the distinct minima in the χ^2 surface for buffers A and B indicate that the difference in K_{MD} is significant. Hence, the dimer is slightly more stable in the presence of magnesium. The free energy difference ΔG derived from the dissociation constants (Table 1) corresponds to 16 and 19 kJ/mol in buffers A and B, respectively. A very similar value was

dx.doi.org/10.1021/ja207742q | J. Am. Chem.Soc. 2012, 134, 1019−1029

Table 1. Rates and Equilibrium Constants of c-di-GMP Oligomerization

	2M ⇄ D
buffer	K_{MD} [10^{-3}M][a]
A (EDTA)	1.3 ± 0.5
B (Mg^{2+})	0.52 ± 0.01
C (TRIS)	>10

	4M ⇄ T		
	k_{TM} [$10^{5}M^{-3}$ s^{-1}]	k_{MT} [$10^{-6}s^{-1}$]	K_{MT} [$10^{-12}M^{3}$]
A (EDTA)[b]	5.6 ± 0.9	4.2 ± 0.3	6.8 ± 0.5
A (EDTA)[c]	3.8	2.6	6.8[d]

	T + 4M ⇄ O		
	k_{OT} [10^{12} M^{-4} s^{-1}]	k_{TO} [$10^{-5}s^{-1}$]	K_{TO} [$10^{-17}M^{4}$]
A (EDTA)[b]	2.4 ± 0.2	5.4 ± 0.3	2.1 ± 0.1
A (EDTA)[c]	3.4	7.1	2.1[d]

[a]Equilibrium constants determined from MD ^{1}H8 chemical shift and peak intensities (Figure 3). [b]M ⇄ T and T ⇄ O reaction parameters derived from the fit of the kinetic model (Figure 6) to the oligomer reassociation experiment in buffer A (Figure 4). [c]M ⇄ T and T ⇄ O reaction parameters derived from the fit of the kinetic model (Figure 6) to the oligomer dissociation experiment in buffer A (Figure 5). [d]Parameter kept fixed during fit.

obtained in a recent molecular dynamics simulation (21 kJ/mol).[14]

In buffer C (TRIS), no resonances other than those belonging to the MD species are observed. Only at concentrations above about 1 mM, the H8 resonance starts to shift significantly (Figures 2C and 3A, crosses) due to the accumulation of dimer, which is in fast exchange with the monomer. However, even at 10 mM concentration, the shift change is not very pronounced, and no convergence to the dimer is achieved. Thus, under these conditions, K_{MD} is significantly higher than 10 mM. This is consistent with a recent report that c-di-GMP is monomeric at 1.0 mM concentration in the absence of metal ions.[19] However, in the latter study the possibility of fast chemical exchange had not been considered.

Under all our buffer conditions, very similar equilibrium constants were obtained when H1′ instead of H8 proton resonances were used for the quantitative evaluation (Figure S7, Table S8).

Higher c-di-GMP Oligomers. Consistent with the previously observed metal-ion-dependent polymorphism[21] at millimolar c-di-GMP concentrations, several sets of resonances become visible at concentrations above about 100 μM (Figure 2A,B). Two sets of these resonances were previously attributed to two separate tetramers of two parallel, but not stacked, G-quartets, each (Figure 1C) with the nucleotides in either all-*syn*

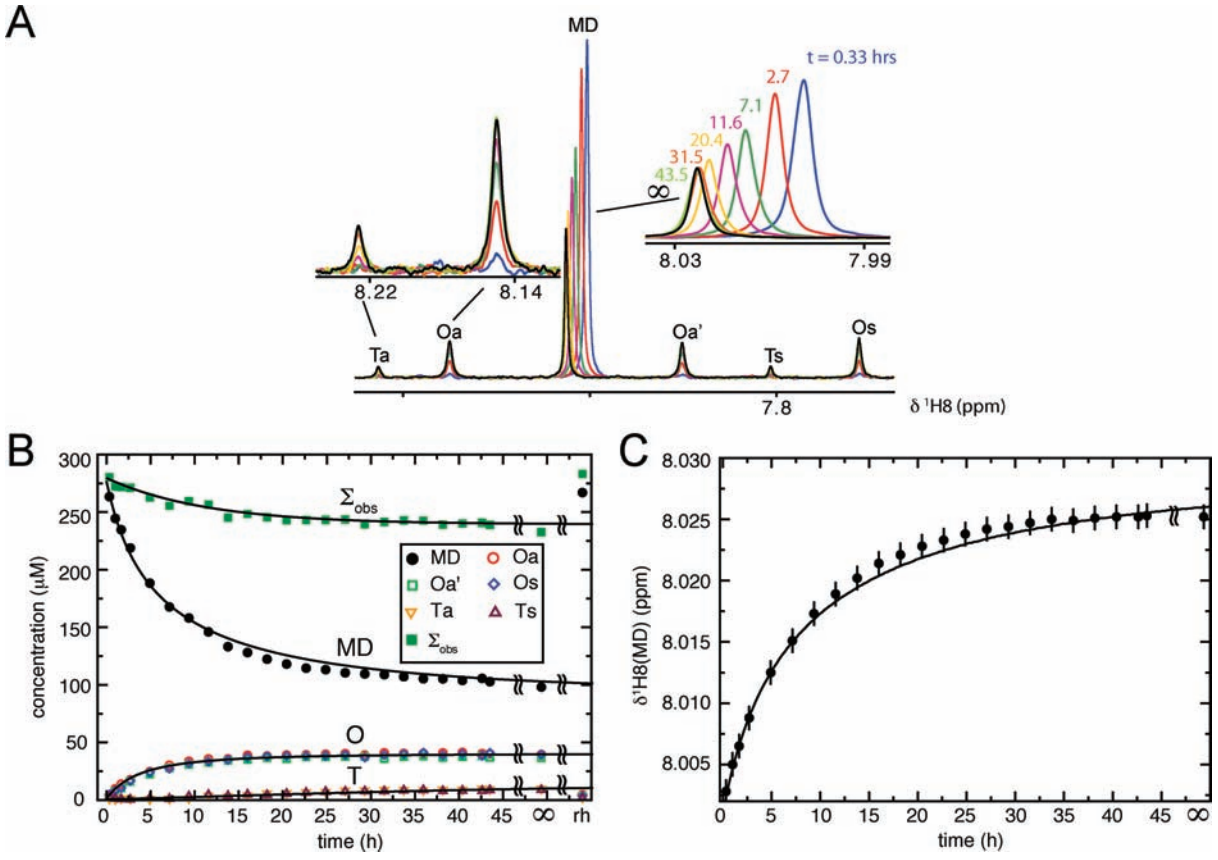

Figure 4. C-di-GMP oligomer reassociation after heat dissociation. (A) Time series of ^{1}H NMR spectra of a 280 μM c-di-GMP sample in buffer A at 24 °C after heat treatment at 60 °C for 1 h. Insets show enlargements of some of the peaks. (B) H8 proton concentrations of the various oligomeric species (symbols) obtained from the corresponding 1D NMR resonance intensities in (A) as a function of time after heating. Continuous lines are fits according to the kinetic model described in the text. An additional point acquired after reheating of the sample to 60 °C for 1.5 h is labeled as "rh". (C) Chemical shift values of the H8 MD resonance (symbols) as a function of time after heating. The continuous line indicates the fit according to the kinetic model shown in Figure 6. For kinetic parameters, see Table 1.

dx.doi.org/10.1021/ja207742q | J. Am. Chem.Soc. 2012, 134, 1019–1029

(Ts) or all-*anti* (Ta) conformation based on H1′ to H8 NOE crosspeaks.[21] Throughout the examined concentration range and also during the two independent kinetic experiments (see below, Figures 4 and 5), the intensities of these resonances remained virtually identical between the two sets (Figure S2A). Virtually equal intensities were also observed during titration and kinetic experiments among the three sets of resonances previously attributed to several octamer structures (Figures 2A,B, 4, 5). On the basis of NOE data, they were identified as all-*syn* (Os) and all-*anti* (Oa/Oa′) octamer conformations, respectively.[21] The very similar intensities for the tetramer and octamer subspecies under all our experimental conditions may indicate subconformations of the same tetramer and octamer complexes rather than completely distinct molecular complexes. In contrast to our observations, unequal intensities of oligomer resonances (Ts vs Ta and Os vs Oa/Oa′) were observed in a recent study on thiophosphate analogues of c-di-GMP under different buffer conditions.[36] In the absence of fully determined tetramer and octamer structures, this issue is unresolved. Besides the tetramer and octamer resonances, additional sets of peaks appear at concentrations above 3 mM (Figure S3). Very likely, these correspond to even higher oligomers. In contrast, at very low concentrations (<∼20 μM) and under all buffer conditions, only the set of MD peaks is observed, shifted almost completely to the monomeric form.

Oligomer Reassociation after Heat Dissociation. The higher oligomers are heat-sensitive and dissociate at an elevated temperature of 60 °C (Figure S4). This provides a convenient means to study the association kinetics of oligomers in a temperature-jump experiment. For this, a 280 μM c-di-GMP sample dissolved in buffer A was heated in a water bath to 60 °C for 1 h and subsequently inserted into the magnet at 24 °C. Figure 4A shows the following slow buildup of the tetramer and octamer peaks in the 1D NMR spectra. At the same time, the MD peak decreases in intensity and shifts downfield, i.e., toward the monomer. The equilibrium is reached only after more than 24 h (Figure 4B,C). Notably, formation of octamers is considerably faster than the formation of tetramers.

Interestingly, the total sum of the H8 peak integrals of the identified species, $\sum_{obs}$, decreased by about 10% over several days and then remained constant for over 6 months (Figure 4B). No precipitation was observed. The effect was not due to an underestimation of the higher oligomer peak intensities resulting from their larger T_1 times, since an extended recovery delay of 62 s (instead of 3 s) yielded identical results. Furthermore, the effect could be reversed by heating to 60 °C (Figure 4B). This is consistent with the reversible formation of even higher oligomeric species, which were below the detection limit of the NMR spectra.

In addition, we checked the changes of oligomer concentrations upon heating an equilibrated sample (280 μM, buffer A) from 297 to 308 K. Consistent with the observation of oligomer dissociation at higher temperatures, the octamer intensities decrease, whereas tetramer intensities first increase and then decrease. The MD resonance gains intensity and shifts toward the dimer, in agreement with the dissociation of the higher oligomeric species. Even after more than 2 h, equilibrium was not reached after the temperature jump. These results indicate that, at higher physiological temperatures in living systems, such as 310 K, c-di-GMP oligomers are even less abundant than at room temperature.

Oligomer Dissociation upon Dilution. Often dilutions from high-concentration stock solutions are used for *in vitro* c-di-GMP enzymatic or biological assays, and it is tacitly assumed that equilibrium is attained immediately. In order to monitor the kinetics of oligomer dissociation under such conditions, a 25 μM c-di-GMP sample in buffer A was prepared by dilution from an equilibrated 1.25 mM stock solution (297 K), and a series of 1D NMR spectra was acquired as a function of time after dilution (Figure 5A,B). As expected, after dilution the MD peak intensity increases and its position shifts toward the dimer, indicative of an increase in total MD concentration and relative dimer population. However, the increase in MD concentration is rather slow and only saturates after about 100 h. Simultaneously, the octamer population decreases continuously, while the tetramer population first increases and then after a period of about 12 h decreases. Several days later, both tetramer and octamer peaks have disappeared completely. This kinetic behavior suggests that tetramers are intermediates of the octamer dissociation reaction. Again, as for the temperature-jump experiment, the total sum of identified peak intensities $\sum_{obs}$ does not remain constant, but in this case increases slightly over time. This is again consistent with invisible higher aggregates at higher concentration that dissociate into observable species upon dilution.

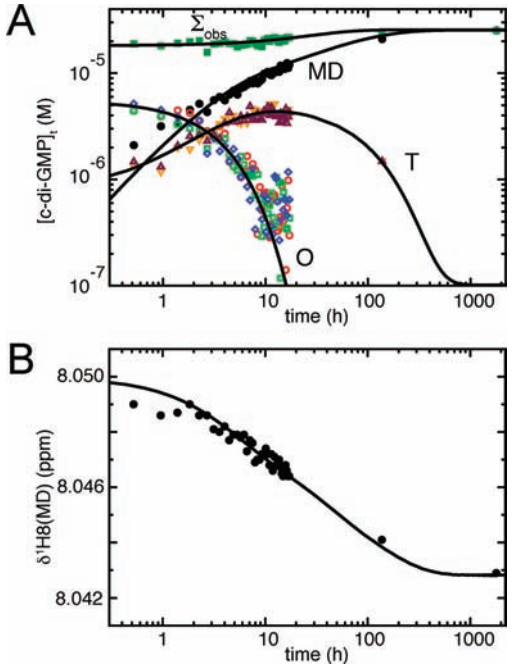

Figure 5. C-di-GMP oligomer dissociation upon dilution. A times series of ^{1}H NMR spectra was recorded on a sample of 25 μM c-di-GMP after dilution from a 1.25 mM stock solution in buffer A. (A) Data points represent experimentally determined concentrations of various c-di-GMP species as a function of time (symbols as in Figure 4). The continuous lines represent the fit according to the kinetic model. (B) Chemical shift of the H8 MD resonance (symbols) with fitted values (continuous line). Experimental chemical shift errors are not larger than 1 ppb.

The slow kinetics upon dilution at ambient temperatures constitutes a problem for biological assays, if care is not taken to reach equilibrium. Procedures for annealing have been proposed, such as a heating−cooling cycle of 95 °C (5 min) to room temperature (15 min) followed by storage in the refrigerator at 4 °C (12 h).[24] Since oligomers are stabilized at low temperatures, we rather propose to keep the sample at the

dx.doi.org/10.1021/ja207742q | J. Am. Chem.Soc. 2012, 134, 1019−1029

measurement temperature after a suitable high-temperature annealing step. The exact duration and temperature may depend on the buffer conditions and c-di-GMP concentration, and equilibration should be assessed experimentally, e.g., by NMR or UV (see below). For a typical situation, we found that incubation at 60 °C (buffer A) of a 25 μM sample dissolved from a 1.3 mM stock solution dissociates 85% of the higher oligomers to monomers and dimers within 1 h, and any higher oligomers are below the detection limit after 2 h (data not shown).

Kinetic Model of c-di-GMP Self-Association. The experimental results can be integrated into a quantitative framework with predictive power by a simple kinetic model of c-di-GMP oligomerization (Figure 6). As shown above,

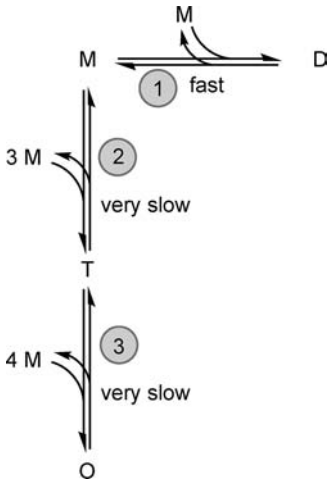

Figure 6. Kinetic scheme of c-di-GMP oligomer formation. M, monomer; D, dimer; T, tetramer; O, octamer.

monomers and dimers are rapidly interconverting. Very likely, the dimer is composed of self-intercalated monomers with stacked bases, as observed in c-di-GMP crystals and in complex with proteins (Figure 1B). Assembly of the hollow-formed tetramer with two nonstacked G-quartets (Figure 1C) would proceed via sequential alignment of monomers in an overall fourth-order reaction. The intercalated dimer is incompatible with such a proposed tetramer structure, since the intercalation would block G-quartet formation. For the assembly of the putative intercalated octamer (Figure 1D), we assume that monomers have to insert sequentially into a preformed tetramer. Note that the intercalated dimer is also not directly compatible with the intercalated octamer structure, since the relative orientation of the monomer subunits changes by about 90° from the dimer to the octamer. Thus, the intercalated dimer may not be directly involved in the formation of the proposed tetramers and octamers. For these reasons, our kinetic model (Figure 6) involves only three reactions (M ⇄ D, M ⇄ T, T ⇄ O), each with a forward and a backward rate (k_{BA} and k_{AB}, respectively) from which the corresponding dissociation constants $K_{AB} = k_{AB}/k_{BA}$ can be derived. Fitting the experimental data to the kinetic model yielded the kinetic parameters for the oligomer equilibria. Since no experimental kinetic data exist for the fast monomer/dimer exchange, the M ⇄ D reaction was treated in the fit as in instant equilibrium according to the dimer dissociation constant K_{MD} determined from the concentration-dependent shift of the MD peak position (see above). The results of the fit to the time-dependent oligomer concentrations of the temperature-jump reassociation experiment are shown in Figure 4B. Taking into account the complication from the decrease in total identified species concentration, $\sum_{obs}$, the fit of the data is quite satisfactory. Further confidence in the kinetic model and the kinetic parameters was obtained from an equally good fit to the dilution experiment data (Figure 5), which yielded very similar rate constants.

The resulting kinetic parameters and equilibrium constants are listed in Table 1. It is apparent that the octamer dissociation rate k_{TO} is below 10^{-4} s^{-1}, i.e., extremely slow. This may be explained by the tight integration of each monomer within the octamer, since each of the two guanine bases of one monomer forms four H-bonds with neighbors in the G-quartets. The same is true for tetramer dissociation, for which an even slower dissociation rate ($k_{MT} < 10^{-5}$ s^{-1}) is found.

With a quantitative model of c-di-GMP oligomerization established that describes the observed data, the concentration of the various species can be calculated as a function of total c-di-GMP concentration. Figure 7 shows that, up to a

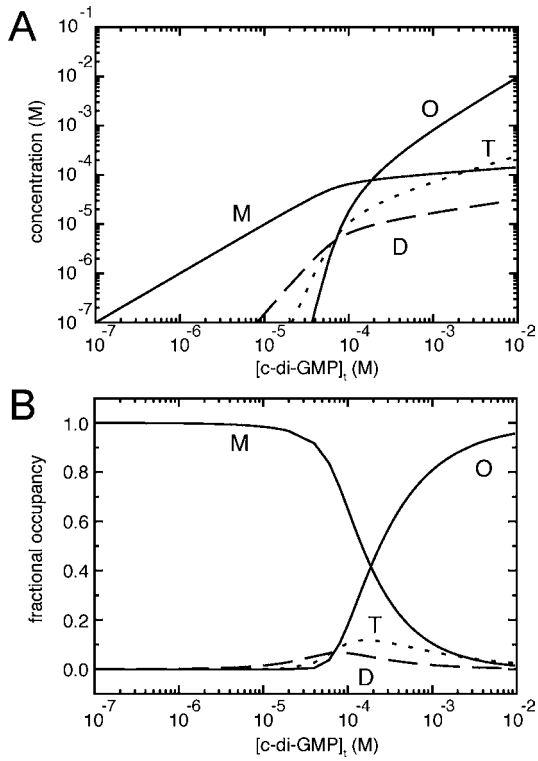

Figure 7. Concentrations of the various oligomeric species of c-di-GMP as a function of total c-di-GMP concentration. (A) Concentrations of the indicated c-di-GMP species (in monomeric units of c-di-GMP) as a function of total c-di-GMP concentration in buffer A. The data were simulated according to the kinetic model shown in Figure 6 with parameters of Table 1. (B) Fractional occupancy of the different species as a function of total c-di-GMP concentration in buffer A.

concentration of about 10 μM, virtually only monomers are present. On a further increase of concentration, dimers start to build up, but only to about 10% of the total population, before octamer formation sets in at about 100 μM. Tetramers, as intermediates to octamer formation, are populated only to a low extent.

dx.doi.org/10.1021/ja207742q | J. Am. Chem.Soc. 2012, 134, 1019–1029

It has also been reported that aromatic compounds may induce oligomer formation.[6,24,25] This conclusion was obtained on the basis of changes in CD, fluorescence, and absorbance spectra. However, no NMR analysis was carried out. To test for such an induced quadruplex formation, we have repeated some of our measurements in the presence of acriflavin/proflavin (Figure S11), which were also used by Sintim and colleagues.[25] After addition of the dye (16 μM), indeed a significant decrease in c-di-GMP (25 μM) MD intensity (H8, H1′) is observed. However, no new signals can be detected that would match the described dimer, tetramer or octamer resonances. In particular, also no H1 resonances are detected that would indicate H-bond formation. We interpret this observation as a possible stacking reaction between dye and c-di-GMP that, however, does not lead to the canonical H-bonded c-di-GMP dimers, tetramers, or octamers.

General considerations[1] and measurements[2] indicate that the overall concentration of c-di-GMP in the bacterial cell is in the 50 nM to a few μM range. Local c-di-GMP pools with higher concentrations have been discussed[1,37] but so far remain hypothetical. Under our buffer conditions, such low concentrations would imply a monomeric form of c-di-GMP. Clearly, intracellular stacking complexes with aromatic compounds cannot be excluded. However, in the absence of such heteromeric stacking reactions, c-di-GMP should be monomeric under *in vivo* conditions. In this respect it is important to note that c-di-GMP adopts a dimeric, self-intercalated form in complex with several proteins, such as diguanylate cyclase,[9,10] a response regulator,[13] and the PilZ receptor.[12] It may be possible that *in vivo* such complexes are formed by the consecutive binding of two monomeric ligands, i.e., that dimerization occurs only on the protein. The conserved intercalation of aromatic and arginine amino acids into the c-di-GMP dimer in the protein complexes[12] may act as a template for the formation of such dimers at low c-di-GMP concentrations.

Assessment of c-di-GMP Association from UV Spectra. Concentration- and temperature-dependent changes in the absorptivity of c-di-GMP have been reported and attributed to the hypochromic effect caused by base stacking.[38] For convenient absorption measurement (OD_{253} < 1), c-di-GMP is usually diluted from millimolar stock solutions to few tens of micromolar concentration. However, due to the very slow kinetics of oligomer dissociation this procedure may leave the solution in an undefined state with varying absorbance properties. As described above, the problem can be overcome by annealing. Once the higher oligomers are dissociated, base stacking in the dimer will only minimally influence the absorption measurement below about 50 μM, since the monomer/dimer dissociation constants are above 0.5 mM, even in the presence of metal ions. No such problems from oligomerization are expected in the absence of metal ions (e.g., TRIS, buffer C), where no higher oligomers are present up to a concentration of at least 10 mM and where the monomer/dimer dissociation constant is even larger. Indeed, Figure S5 demonstrates that Lambert–Beer's law is obeyed perfectly in buffer C, and a molar extinction coefficient was determined at the absorption maximum of 253 nm as ε_{253}(c-di-GMP) = (28.6 ± 1.0) × 10^3 M^{-1} cm^{-1} by a combination of absorption and NMR intensity measurements that were calibrated to a reference GTP sample (see Materials and Methods). The form of the absorption spectrum of c-di-GMP under these conditions is virtually identical to that of GTP, and not surprisingly ε_{253}(c-di-GMP) is very close to twice the value for GTP[32] (13.7 × 10^3 M^{-1} cm^{-1}), indicating that the two guanine bases in monomeric c-di-GMP are not strongly interacting.

In contrast to the absorption spectrum of monomeric c-di-GMP, the spectra of its oligomeric forms differ from that of GTP (Figure 8). The base stacking causes both a decrease in the amplitude (hypochromicity) and a red shift (bathochromicity) of the guanine spectrum. Figure 8A shows this effect in time-dependent absorption spectra of 25 μM c-di-GMP recorded at 24 °C after dilution into buffer A from a 1.25 mM stock solution. Initially, the spectrum has a main maximum at 256 nm and a second shoulder at 295 nm. With increasing time, the absorption shifts to the blue and increases to converge toward the GTP spectrum with a main maximum at 253 nm and the second shoulder at 280 nm. This behavior can be described quantitatively to a good approximation by a linear superposition of a monomeric (unstacked) and a stacked spectral species, where the time-dependent population of the monomeric form is determined from the intensity and position

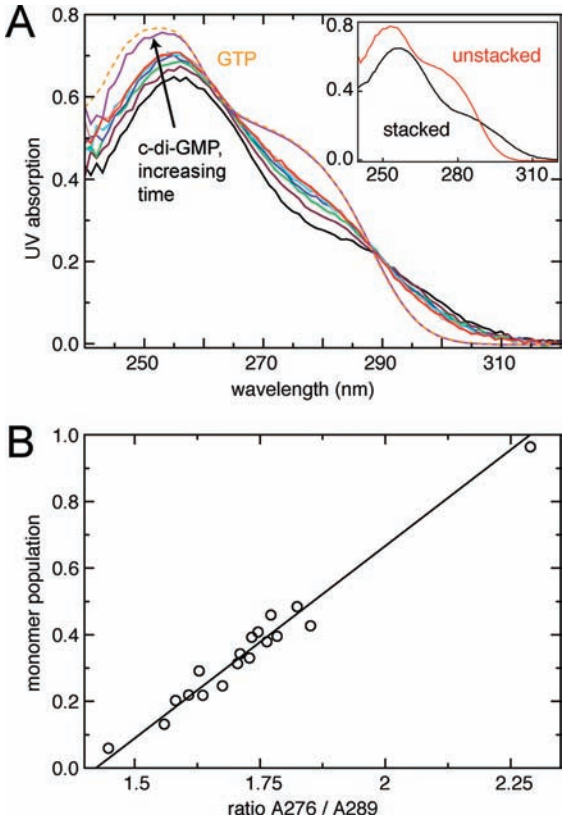

Figure 8. UV analysis of the aggregation state of c-di-GMP. (A) Time course of UV absorption spectra of 25 μM c-di-GMP after dilution into buffer A. Colors present spectra recorded at different times: 10 min (black), 190 min (maroon), 370 min (green), 550 min (blue), 730 min (cyan), 910 min (brown), 970 min (red), and 75 days after dilution (violet). For comparison, the absorption spectrum of GTP (scaled according to its NMR peak intensity relative to that of c-di-GMP) is shown (orange, dashed). The inset shows the deconvoluted spectra for unstacked (black) and stacked (red) species. (B) Population of monomeric c-di-GMP p_{mono} as a function of the UV absorption ratio of 276/289 nm (isosbestic point, 288.8 nm). The monomeric populations were obtained from the NMR dilution experiment (Figure 5). The solid line indicates a linear fit of the form p_{mono} = 1.15 (A_{276}/A_{289}) − 1.64.

dx.doi.org/10.1021/ja207742q | J. Am. Chem.Soc. 2012, 134, 1019–1029

of the H8 resonance in a ^{1}H spectrum recorded on the same sample. A linear fit according to eq 6 yields predicted time-dependent spectra, which are almost indistinguishable from the experimental data (Figure S6). The decomposed monomeric (unstacked) and stacked spectra according to the fit are shown in Figure 8A. The spectrum of the unstacked form is identical to the GTP spectrum with a maximum at 253 nm, whereas the spectrum of the stacked form has an about 16% lower maximal extinction at 256 nm. The isosbestic point is located at 288.8 nm. For accurate determination of the total concentration in the presence of stacking, it is thus advisible to use the absorbance at the isosbestic point.

Figure 8A shows that the maximal difference between monomeric and stacked species occurs at 276 nm. The ratio of the absorbance at this wavelength to the absorbance at the isosbestic point (A_{276}/A_{289}) may be taken as a measure for the relative monomer population p_{mono}. Indeed, an excellent linear correlation is observed (Figure 8B). Thus the absorbance ratio A_{276}/A_{289} provides an easy measure of the dissociation state.

CONCLUSION

Due to the propensity of base-stacking and G-quartet formation, c-di-GMP can display a rich polymorphism of higher oligomeric forms in the presence of metal ions. Besides monomers and dimers, at least two forms of guanosines in putative tetramer and three forms in putative octamer structures are distinguishable in ^{1}H proton NMR spectra at low millimolar concentrations. In this study, we have determined kinetic parameters and equilibrium constants of the interchange between these different forms.

Dissociation constants of the dimer are on the order of 1 mM in the presence of metal ions but significantly larger in their absence. Irrespective of the presence of metal ions, c-di-GMP exchanges rapidly between monomeric and dimeric forms on the chemical shift time scale of milliseconds. Higher oligomer formation occurs only in the presence of monovalent (particularly K^+) metal ions. The two forms of guanosines in tetramers and the three forms in octamers are always found in equal concentration presumably because these oligomers contain distinct guanosine subconformations within the same molecule. In contrast to the dimerization reaction, the kinetics of higher oligomer formation and dissociation is extremely slow and can require weeks to reach equilibrium. The kinetics of monomer, dimer, tetramer, and octamer exchange can be described to good quantitative agreement by a simplified model where the tetramer is an intermediate of octamer formation.

The extremely slow dissociation kinetics of the higher oligomers may lead to artifactual low concentrations of the active monomeric form when c-di-GMP is diluted from concentrated stock solutions in biological assays. The problem can be overcome by an annealing step, e.g., incubation at 60 °C for more than 2 h. Since the base stacking associated with oligomer formation causes a red shift of the UV spectra, the proper monomer content can be verified easily from the UV absorption ratio (A_{276}/A_{289}).

Under all tested buffer conditions, c-di-GMP was monomeric at low micromolar concentrations, in particular also at very high potassium concentrations that favor higher homooligomer formation. Although it cannot be excluded that aromatic compounds may serve as templates for other types of higher oligomers in the complex environment of a biological cell, it is unlikely that homooligomeric structures in free form are populated to a significant extent at the low cellular c-di-GMP concentrations.

ASSOCIATED CONTENT

Supporting Information

1D NMR spectra of c-di-GMP under various buffer and temperature conditions, correlation of UV data with c-di-GMP NMR concentrations in TRIS buffer, fit of the time-dependent UV spectra by two-state model, evaluation of NMR H1′ data, and NMR spectra of GTP. This material is available free of charge via the Internet at http://pubs.acs.org.

AUTHOR INFORMATION

Corresponding Author

stephan.grzesiek@unibas.ch; tilman.schirmer@unibas.ch

Present Address

[§]Harvard Medical School, 240 Longwood Ave., Boston, MA 02115

ACKNOWLEDGMENTS

We thank U. Jenal, D. Häussinger, H.-J. Sass, and D. Samoray for helpful discussions. This work was supported by SNF grants 31-132857 to S.G. and 31-105587 to T.S.

REFERENCES

(1) Hengge, R. *Nat. Rev. Microbiol.* **2009**, *7*, 263.
(2) Simm, R.; Morr, M.; Rerriminghorst, U.; Andersson, M.; Romling, U. *Anal. Biochem.* **2009**, *386*, 53.
(3) Schirmer, T.; Jenal, U. *Nat. Rev. Microbiol.* **2009**, *7*, 724.
(4) Kim, D.; Hunt, J. F.; Schirmer, T. In *The Second Messenger Cyclic Di-GMP*; Wolfe, A. J., Visick, K. L., Eds.; John Wiley & Sons: New York, 2010; p 76.
(5) Egli, M.; Gessner, R. V.; Williams, L. D.; Quigley, G. J.; Vandermarel, G. A.; Vanboom, J. H.; Rich, A.; Frederick, C. A. *Proc. Natl. Acad. Sci. U.S.A.* **1990**, *87*, 3235.
(6) Liaw, Y. C.; Gao, Y. G.; Robinson, H.; Sheldrick, G. M.; Sliedregt, L.; Vandermarel, G. A.; Vanboom, J. H.; Wang, A. H. J. *FEBS Lett.* **1990**, *264*, 223.
(7) Guan, Y.; Gao, Y. G.; Liaw, Y. C.; Robinson, H.; Wang, A. H. J. *J. Biomol. Struct. Dyn.* **1993**, *11*, 253.
(8) Blommers, M. J. J.; Haasnoot, C. A. G.; Walters, J.; Vandermarel, G. A.; Vanboom, J. H.; Hilbers, C. W. *Biochemistry* **1988**, *27*, 8361.
(9) Chan, C.; Paul, R.; Samoray, D.; Amiot, N. C.; Giese, B.; Jenal, U.; Schirmer, T. *Proc. Natl. Acad. Sci. U.S.A.* **2004**, *101*, 17084.
(10) De, N.; Pirruccello, M.; Krasteva, P. V.; Bae, N.; Raghavan, R. V.; Sondermann, H. *PLoS Biol.* **2008**, *6*, 601.
(11) Ko, J.; Ryu, K. S.; Kim, H.; Shin, J. S.; Lee, J. O.; Cheong, C.; Choi, B. S. *J. Mol. Biol.* **2010**, *398*, 97.
(12) Habazettl, J.; Allan, M. G.; Jenal, U.; Grzesiek, S. *J. Biol. Chem.* **2011**, *286*, 14304.
(13) Krasteva, P. V.; Fong, J. C. N.; Shikuma, N. J.; Beyhan, S.; Navarro, M.; Yildiz, F. H.; Sondermann, H. *Science* **2010**, *327*, 866.
(14) Zhang, L. X.; Meuwly, M. *ChemPhysChem* **2011**, *12*, 295.
(15) Minasov, G.; Padavattan, S.; Shuvalova, L.; Brunzelle, J. S.; Miller, D. J.; Basle, A.; Massa, C.; Collart, F. R.; Schirmer, T.; Anderson, W. F. *J. Biol. Chem.* **2009**, *284*, 13174.
(16) Barends, T. R. M.; Hartmann, E.; Griese, J. J.; Beitlich, T.; Kirienko, N. V.; Ryjenkov, D. A.; Reinstein, J.; Shoeman, R. L.; Gomelsky, M.; Schlichting, I. *Nature* **2009**, *459*, 1015.
(17) Navarro, M. V. A. S.; De, N.; Bae, N.; Wang, Q.; Sondermann, H. *Structure* **2009**, *17*, 1104.
(18) Benach, J.; Swaminathan, S. S.; Tamayo, R.; Handelman, S. K.; Folta-Stogniew, E.; Ramos, J. E.; Forouhar, F.; Neely, H.; Seetharaman, J.; Camilli, A.; Hunt, J. F. *EMBO J.* **2007**, *26*, 5153.
(19) Wang, J.; Zhou, J.; Donaldson, G. P.; Nakayama, S.; Yan, L.; Lam, Y.-f.; Lee, V. T.; Sintim, H. O. *J. Am. Chem. Soc.* **2011**, *133*, 9320.

(20) Zhang, Z.; Gaffney, B. L.; Jones, R. A. *J. Am. Chem. Soc.* **2004**, *126*, 16700.
(21) Zhang, Z.; Kim, S.; Gaffney, B. L.; Jones, R. A. *J. Am. Chem. Soc.* **2006**, *128*, 7015.
(22) Mooren, M. M. W.; Wijmenga, S. S.; Vandermarel, G. A.; Vanboom, J. H.; Hilbers, C. W. *Nucleic Acids Res.* **1994**, *22*, 2658.
(23) Phillips, K.; Dauter, Z.; Murchie, A. I.; Lilley, D. M.; Luisi, B. *J. Mol. Biol.* **1997**, *273*, 171.
(24) Nakayama, S.; Kelsey, I.; Wang, J. X.; Roelofs, K.; Stefane, B.; Luo, Y. L.; Lee, V. T.; Sintim, H. O. *J. Am. Chem. Soc.* **2011**, *133*, 4856.
(25) Nakayama, S.; Kelsey, I.; Wang, J. X.; Sintim, H. O. *Chem. Commun.* **2011**, *47*, 4766.
(26) Lane, A. N.; Chaires, J. B.; Gray, R. D.; Trent, J. O. *Nucleic Acids Res.* **2008**, *36*, 5482.
(27) Murshudov, G. N.; Vagin, A. A.; Dodson, E. J. *Acta Crystallogr. D* **1997**, *53*, 240.
(28) Zaehringer, F.; Massa, C.; Schirmer, T. *Appl. Biochem. Biotechnol.* **2011**, *163*, 71.
(29) Sundararaj, S.; Guo, A.; Habibi-Nazhad, B.; Rouani, M.; Stothard, P.; Ellison, M.; Wishart, D. S. *Nucleic Acids Res.* **2004**, *32*, D293.
(30) Hwang, T. L.; Shaka, A. J. *J. Magn. Reson. Ser. A* **1995**, *112*, 275.
(31) Wider, G.; Dreier, L. *J. Am. Chem. Soc.* **2006**, *128*, 2571.
(32) Bock, R. M.; Ling, N. S.; Morell, S. A.; Lipton, S. H. *Arch. Biochem. Biophys.* **1956**, *62*, 253.
(33) Gilbert, D. E.; Feigon, J. *Curr. Opin. Struct. Biol.* **1999**, *9*, 305.
(34) Ida, R.; Wu, G. *J. Am. Chem. Soc.* **2008**, *130*, 3590.
(35) Ida, R.; Kwan, I. C. M.; Wu, G. *Chem. Commun.* **2007**, 795.
(36) Zhao, J. W.; Veliath, E.; Kim, S.; Gaffney, B. L.; Jones, R. A. *Nucleosides Nucleotides Nucleic Acids* **2009**, *28*, 352.
(37) Römling, U.; Gomelsky, M.; Galperin, M. Y. *Mol. Microbiol.* **2005**, *57*, 629.
(38) Danilov, V. I. *FEBS Lett.* **1974**, *47*, 155.